Hindawi Publishing Corporation
Advances in Acoustics and Vibration
Volume 2014, Article ID 401042, 7 pages
http://dx.doi.org/10.1155/2014/401042

Research Article

S_1-ZGV Modes of a Linear and Nonlinear Profile for Functionally Graded Material Using Power Series Technique

M. Zagrouba,[1] M. S. Bouhdima,[1,2] and M. H. Ben Ghozlen[1]

[1] *Laboratory of Physics Materials, Faculty of Sciences, University of Sfax, B.P. 1171, 3000 Sfax, Tunisia*
[2] *Superior Institute of Applied Science and Technology, University of Gabes, 6072 Zrig, Gabes, Tunisia*

Correspondence should be addressed to M. S. Bouhdima; m.bouhdima@yahoo.fr

Received 14 May 2014; Revised 24 July 2014; Accepted 5 August 2014; Published 21 September 2014

Academic Editor: Rama B. Bhat

The present work deals with functionally graded materials (FGM) isotropic plates in the neighborhood of the first-order symmetric zero group velocity (S_1-ZGV) point. The mechanical properties of functionally graded material (FGM) are assumed to vary continuously through the thickness of the plate and obey a power law of the volume fraction of the constituents. Governing equations for the problem are derived, and the power series technique (PST) is employed to solve the recursive equations. The impact of the FGM basic materials properties on S_1-ZGV frequency of FGM plate is investigated. Numerical results show that S_1-ZGV frequency is comparatively more sensitive to the shear modulus. The gradient coefficient p does not affect the linear dependence of ZGV frequency f_o as function of cut-off frequency f_c; only the slope is slightly varied.

1. Introduction

A functionally graded material (FGM) is a kind of an inhomogeneous material. The characterization of mechanical properties of materials is important for testing their structural integrity. Lamb waves are frequently employed in the ultrasonic characterization of thin plates [1]. As an important property of Lamb waves, the zero group velocity (ZGV) at the frequency minimum f_o of the first-order symmetric (S_1) continues to be of an interest for the scientific community [2, 3]. Tolstoy and Usdin pointed out that for the S_1 Lamb mode, group velocity vanishes at a particular point of the dispersion curve and predicted that this zero group velocity point must be associated with a sharp continuous wave resonance and ringing effect [4]. Holland and Chimenti demonstrated the exploitation of this mode for high-sensitivity imaging applications. With air-coupled transducers, they observed the transparency of a plate due to the S_1 mode ZGV resonance [5].

The S_1-ZGV frequency is obviously sensitive to mechanical properties and to any change in the plate thickness. To exploit this phenomenon recent works evoke the idea that it may be suitable for the measurement of nanometer-scale thickness variations in homogeneous plates [6, 7]. Due to the resulting differential equations of variable coefficients associated with the spatial variation of the material properties, the wave propagation in FGM remains difficult to analyze. Some numerical [8–10] and analytical methods [11–16] have been applied in order to study the wave propagation behavior in an inhomogeneous medium with material properties varying continuously along the depth direction. In an effort to show the interest of ZGV in the study of FGM materials, Bouhdima [15] first discussed the effect of the linear variation of mechanical properties along the thickness plate on the S_1-ZGV using the power series technique (PST). To our knowledge, no reports have been published on the relationship between the S_1-ZGV frequency and material properties in an inhomogeneous free standing plate. Previous investigations on S_1-ZGV phenomenon are limited to inspection experiments on homogenous plates and mainly focused on measuring the thickness of a coating on a relatively thin plate [3, 7, 17]. The present investigation includes different kinds of FGM plates with various basic materials, to extract the effects produced by mechanical parameters variation. All the selected materials for the illustration are in agreement with the convergence criterion. The PST has been used and the recursive relationship

for $p = 2$ is derived. The performed developments permit the evaluation of the impact of the nonlinear profile on dispersion curves of Lamb waves. The effect of the shear modulus on this frequency is highlighted. Furthermore, the relative variation of the stress and the mechanical displacement is investigated at the S_1-ZGV frequency.

The FGM plate data and the basic theory of PST are reported in Sections 2-3. The last paragraph is devoted to the discussion and the main results.

2. Statement of the Problem and Theoretical Study

A functionally graded plate with thickness "d" is considered here. It is assumed that the mechanical properties of FGM vary continuously through the thickness of plate. The motion is restricted in the (x_1, x_3) plane and the Lamb waves propagate in the positive direction of the x_1-axis. The material properties α can be expressed as [18–21]

$$\alpha\left(x_3\right) = \alpha_c \times F_c + \alpha_m \times F_m, \tag{1}$$

where F_m and F_c are the volume fractions and the subscripts m and c denote the metallic and ceramic constituents, respectively. F_c and F_m follow a simple power law as

$$F_c = \left(\frac{x_3}{d} + \frac{1}{2}\right)^p, \qquad F_m = 1 - F_c, \tag{2}$$

where x_3 is the thickness coordinate and "p" is a gradient coefficient. According to this distribution, the bottom surface ($x_3 = -d/2$) of the functionally graded plate is pure metal and the top surface ($x_3 = d/2$) is pure ceramic, and for different values of "p" one can obtain different volume fractions of metal.

The constitutive equations can be expressed as follows:

$$\begin{aligned} T_{ij} &= C_{ijkl} S_{kl}, \\ S_{ij} &= \frac{1}{2}\left(\frac{\partial u_i}{\partial x_j} + \frac{\partial u_j}{\partial x_i}\right), \\ \frac{\partial T_{ij}}{\partial x_j} &= \rho \times \ddot{u}_i. \end{aligned} \tag{3}$$

In (3), T_{ij} and S_{kl} are the stress and strain tensors, C_{ijkl} are the elastic coefficients, ρ is the density, and u_i is the component of the mechanical displacement in the ith direction.

On the basis of the previous assumption of plane strain, the displacement components can be described as

$$\begin{aligned} u_1\left(x_1, x_3, t\right) &= U_1\left(x_3\right) \exp\left[i\left(kx_1 - \omega t\right)\right]; \\ u_2 &= 0; \\ u_3\left(x_1, x_3, t\right) &= iU_3\left(x_3\right) \exp\left[i\left(kx_1 - \omega t\right)\right], \end{aligned} \tag{4}$$

where k is the wave number, ω denotes the frequency, and $i = \sqrt{-1}$. Note that for convenient description i is introduced to make the first and third displacement components in phase quadrature so that the polarization locus becomes elliptical. Additionally the recursive process inherent to the PST method will have a suitable form. On the other hand and for brevity, the complex exponential $\exp[i(kx_1 - \omega t)]$ is omitted below. From (3)-(4), the governing equations in an inhomogeneous FGM plate are rewritten as follows:

$$\begin{aligned} &c_{44}U_1'' + c_{44}'U_1' + \left(\rho\omega^2 - c_{11}k^2\right)U_1 - \left(c_{13} + c_{44}\right)kU_3' \\ &\quad - kc_{44}'U_3 = 0 \\ &c_{11}U_3'' + c_{11}'U_3' + \left(\rho\omega^2 - c_{44}k^2\right)U_3 + \left(c_{13} + c_{44}\right)kU_1' \\ &\quad + c_{13}'kU_1 = 0. \end{aligned} \tag{5}$$

The symbols ($'$) and ($''$) represent the first and second differentials with respect to x_3. The considered FGM materials are isotropic so their elastic constants are expressed in terms of Lame's coefficients λ and μ; this leads to $c_{11} = \lambda + 2 \cdot \mu$, $c_{13} = \lambda$, and $c_{44} = \mu$.

Then (5) can be transformed into the following forms:

$$\begin{aligned} &\mu U_1'' + \mu' U_1' + \left(\rho c^2 - \lambda - 2\mu\right)k^2 U_1 - \left(\lambda + \mu\right)kU_3' \\ &\quad - k\mu' U_3 = 0 \\ &\left(\lambda + 2\mu\right)U_3'' + \left(\lambda + 2\mu\right)'U_3' + \left(\rho c^2 - \mu\right)k^2 U_3 + \left(\lambda + \mu\right)kU_1' \\ &\quad + \lambda' kU_1 = 0. \end{aligned} \tag{6}$$

For Lamb waves that propagate in the FGM plate, the traction free boundary condition should be satisfied at the top and bottom surfaces ($x_3 = \pm d/2$), that is,

$$T_{13}\left(x_3 = \pm\frac{d}{2}\right) = 0, \qquad T_{33}\left(x_3 = \pm\frac{d}{2}\right) = 0. \tag{7}$$

Equations (6) are relative to the motion along x_1 and x_3; they reveal coupling between both displacement amplitudes U_1 and U_3.

3. Used Method

To solve the differential equation with variable coefficients, we use the PST method [15, 16]. Regarding the longitudinal and the shear wave amplitudes for Lamb guided waves, the PST method specifies that U_1 and U_3 can take the following forms:

$$U_1 = \sum_n A_n\left(\frac{x_3}{d}\right)^n; \qquad U_3 = \sum_n B_n\left(\frac{x_3}{d}\right)^n. \tag{8}$$

It is assumed that the parameters of the FGM possess the following form:

$$\lambda(x_3) = \sum_{i=0}^{p} a_i \left(\frac{x_3}{d}\right)^i$$
$$\mu(x_3) = \sum_{i=0}^{p} b_i \left(\frac{x_3}{d}\right)^i \quad (9)$$
$$\rho(x_3) = \sum_{i=0}^{p} c_i \left(\frac{x_3}{d}\right)^i.$$

Substituting (8) and (9) into (6) and by equating the coefficients of $(x_3/d)^n$ to zero we can obtain two recursive equations. At this level any couple (A_n, B_n) can be expressed as a function of the quadruplet $\{A_0, A_1, B_0, B_1\}$; this is true for the displacement components. Accordingly, any physical magnitude will have a four-dimensional vector form. For $p = 2$, the corresponding recursive relationships involving A_n and B_n are written below:

$$\begin{aligned}
&(n+2)(n+1)b_o A_{n+2} + (n+1)^2 b_1 A_{n+1} \\
&\quad - kd(n+1)(a_o + b_o) B_{n+1} \\
&\quad + \left[k^2 d^2 \left(c_o C^2 - a_{oo}\right) + n(n+1) b_2\right] A_n \\
&\quad - kd\left[n a_1 + (n+1) b_1\right] B_n \\
&\quad + k^2 d^2 \left(c_1 C^2 - a_{11}\right) A_{n-1} \\
&\quad - kd\left[(n-1) a_2 + (n+1) b_2\right] B_{n-1} \\
&\quad + k^2 d^2 \left(c_2 C^2 - a_{22}\right) A_{n-2} = 0, \\
&(n+2)(n+1) a_{oo} B_{n+2} + (n+1)^2 a_{11} B_{n+1} \\
&\quad + kd(n+1)(a_o + b_o) A_{n+1} \\
&\quad + \left[k^2 d^2 \left(c_o C^2 - b_o\right) + n(n+1) a_{22}\right] B_n \\
&\quad + kd\left[n b_1 + (n+1) a_1\right] A_n + k^2 d^2 \left(c_1 C^2 - b_1\right) B_{n-1} \\
&\quad + kd\left[(n-1) b_2 + (n+1) a_2\right] A_{n-1} \\
&\quad + k^2 d^2 \left(c_2 C^2 - b_2\right) B_{n-2} = 0
\end{aligned} \quad (10)$$

with $a_{oo} = a_o + 2b_o$, $a_{11} = a_1 + 2b_1$, $a_{22} = a_2 + 2b_2$, k is the wave number, and C is the phase velocity. Some explorations related to coefficients denoted a_i, b_i, c_i $(i = 0, 1, 2)$ are deduced from the properties of the FGM basic materials (see (9)). A_j and B_j are equal to zero if $j < 0$.

The next step consists of putting boundary conditions in a suitable matrix form. Stress components T_{i3} written with respect to $\{A_0, A_1, B_0, B_1\}$ on both sides of the plate give rise to a square matrix (4×4) dependent on ω and k. For a given frequency, the secular equation leads to the corresponding wave number and obviously to the phase velocity. Then, the dispersion curves of symmetric and antisymmetric propagative Lamb modes are represented by a set of branches in the plane (ω, c).

Table 1: The physical properties of basic materials.

Material	λ (Gpa)	μ (Gpa)	ρ (Kg/m^3)	f_o (MHz)
Cu	79.291	37.313	8930	1.17
Ni	133.27	81.679	8907	1.66
Cr	74.2	102.5	7190	1.85
Si	86.1	79.5	2329	3.02
Ceramic	138	118.11	3900	2.87

From the recursive relationships one can deduce the convergence criteria:

$$\lim_{n\to\infty} \frac{A_{n+1}}{A_n} = \frac{b_1}{b_o}, \qquad \lim_{n\to\infty} \frac{B_{n+1}}{B_n} = \frac{a_1 + 2b_1}{a_o + 2b_o}. \quad (11)$$

The convergence condition of the solution is satisfied when $|b_1/b_o| < 1$ and $|(a_1 + 2b_1)/(a_o + 2b_o)| < 1$. That has been checked for the selected basic materials.

4. Results and Discussion

An artificial FGM is composed of two different kinds of material and the volume fraction of each material varies along the thickness [22]. As it is mentioned above and according to (1) and (2), both density and elastic constants of FGM material are functions of x_3 coordinate. The physical properties of basic materials used in this study are shown in Table 1.

In the present work metals are associated either with silicon or ceramic. The linear and nonlinear graded variation of volume fraction of metallic phase through the plate thickness are investigated below on the basis of (1).

Figure 1 shows the variations of volume fraction of metallic phase through the plate thickness for $p = 1$ and 2. When the gradient coefficient p is equal to one, the left side is metal-rich and the right side is ceramic-rich. The F_m parameter gives the mass rate of metal in the FGM plate. Anywhere in the plate the mass rate of metal is increased when $p = 2$ comparatively with $p = 1$. for high values of p, the change trend of properties is more pronounced.

To study the S_1-ZGV modes of the FGM plate, different kinds of FGM are considered. The investigation includes different basic materials; accordingly the nature of the ceramic and/or the nature of metal is changed. The FGMs considered in this study are reminded in Table 2. Similarly their S_1-ZGV frequency f_o and cut-off frequencies f_c are also reported for both cases linear $(p = 1)$ and nonlinear $(p = 2)$.

4.1. Effect of Graded Variation on the S_1-ZGV Mode. The dispersion curves provide information on the properties of materials. Some branches of the dispersion curves exhibit minima for nonzero wave numbers. Such phenomenon has been observed very early for the first-order symmetric (S_1) mode [3–5]. The dispersion curves of Lamb waves in an FGM

Table 2: S_1-ZGV and cut-off frequencies of the different FGMs for $p = 1$ and $p = 2$.

FGM plate	$p = 1$		$p = 2$	
	f_o (MHz)	f_c(MHz)	f_o (MHz)	f_c (MHz)
Cr-ceramic	2.29	2.40	2.15	2.25
Cr-Si	2.30	2.40	2.18	2.28
Ni-ceramic	2.15	2.25	2.00	2.12
Ni-Si	2.14	2.28	2.01	2.14
Cu-ceramic	1.86	1.94	1.59	1.69
Cu-Si	1.80	1.87	1.62	1.71

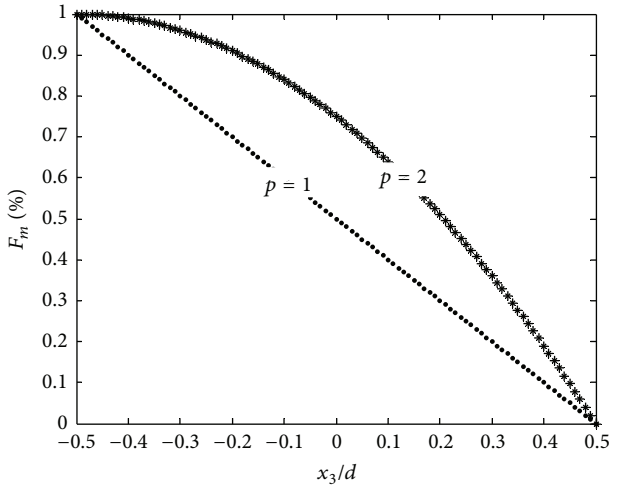

Figure 1: Variations of the volume fraction of metallic phase through the dimensionless thickness of the functionally grated plate.

plate are located between those for the two corresponding homogeneous plates [15, 16] (Figure 2).

The dispersion curves and the S_1-ZGV frequency are influenced not only by the gradient functions but also by the gradient coefficients p. From Figure 3, one can see how the S_1-ZGV frequency is sensitive to the FGM profiles. When p evolves from the linear to nonlinear case an appreciable shift towards lower frequency is observed. In fact, to elucidate our perception of S_1-ZGV modes for linear and nonlinear FGM profile, different basic materials are considered.

The observed shift towards low frequency in the above plot (Cr-ceramic) has been checked for the other couples of basic materials. That shift is expected since nonlinear p corresponds to a FGM plate closer to the metallic phase.

4.2. Influence of Shear Modulus on the S_1-ZGV Frequency. From the investigation of FGM plates, where the ceramic is kept unchanged, one can see from Figure 4(a) that the layout of different dispersion curves for the FGMs plates is coherent with their metals shear modulus ($\mu_{Cu} < \mu_{Ni} < \mu_{Cr}$). Accordingly, the S_1-ZGV frequency value seems to be sensitive to the nature of the metallic component. In the numerical analysis, the variation of metals shear modulus (from 81.7 Gpa to 102.5 Gpa) corresponds to a S_1- ZGV frequency shift about 240 KHz. Conversely the effect of ceramic

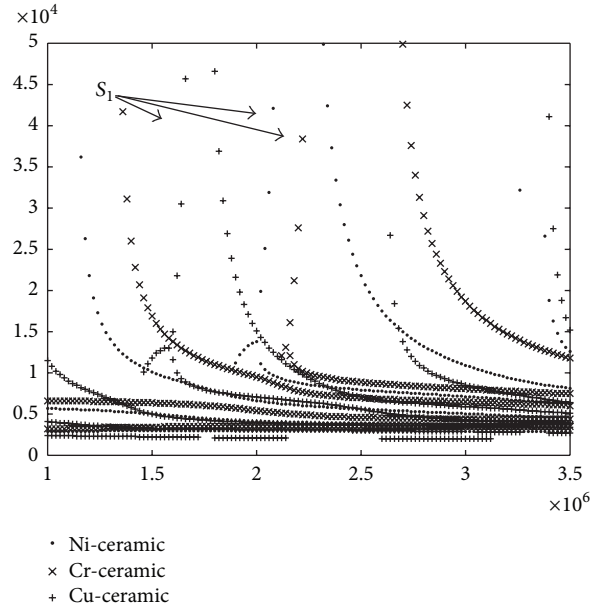

Figure 2: The dispersion curves of Lamb waves in the plates of Cr, FGM and ceramic.

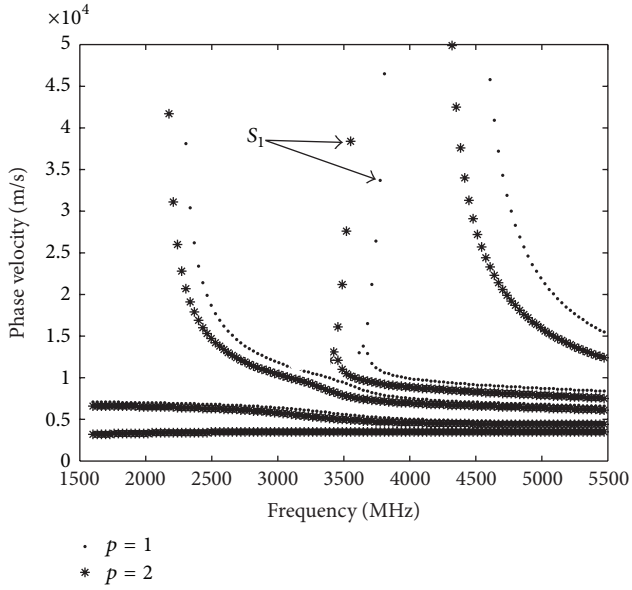

Figure 3: S_1-ZGV frequency shift when p evolves from the linear to nonlinear case.

shear modulus is not so significant (Figure 4(b)). In fact, despite a large deviation of ceramic shear modulus (79.5 GPa for ceramic and 118.1 GPa for Si) the S_1-ZGV frequency shift does not exceed 10 KHz. Such shift increases according to the gradient coefficient p.

Additionally the numerical investigation includes the effect associated with the plate thickness variation from d to $2d$. As it was reported previously in literature [7, 16], the ZGV frequency exhibits a linear behavior with respect to ($d^{-1/2}$).

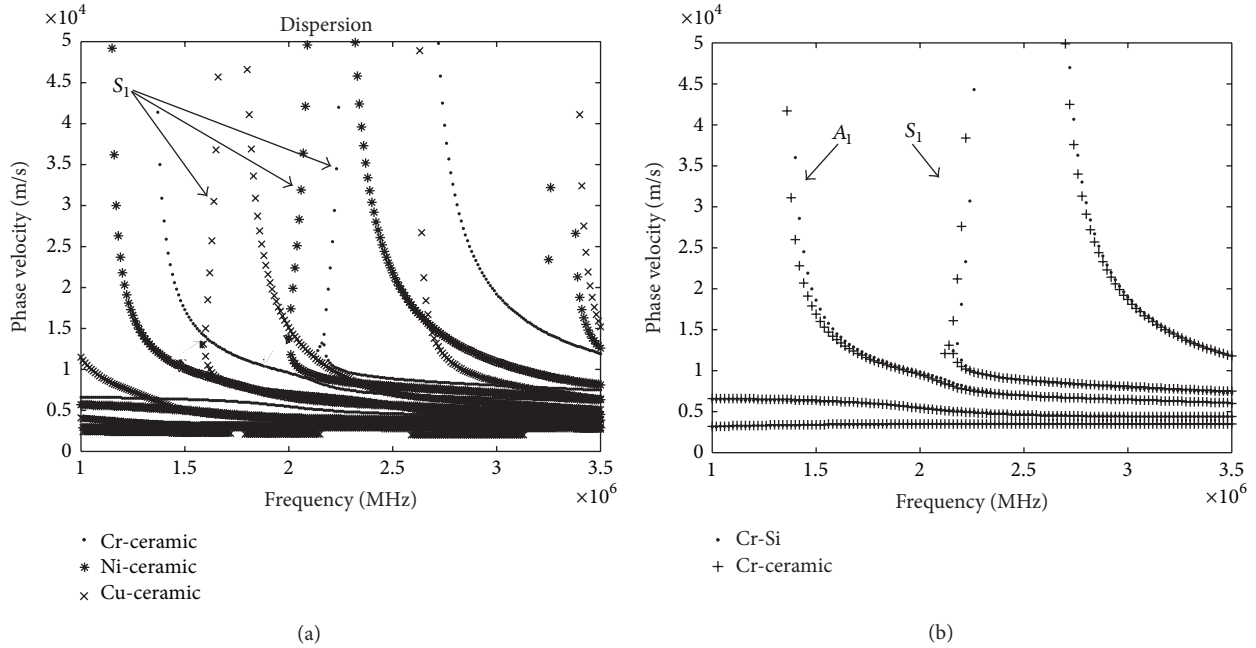

FIGURE 4: Influence of the shear modulus on the S_1-ZGV frequency, (a) metals shear modulus, (b) ceramic shear modulus.

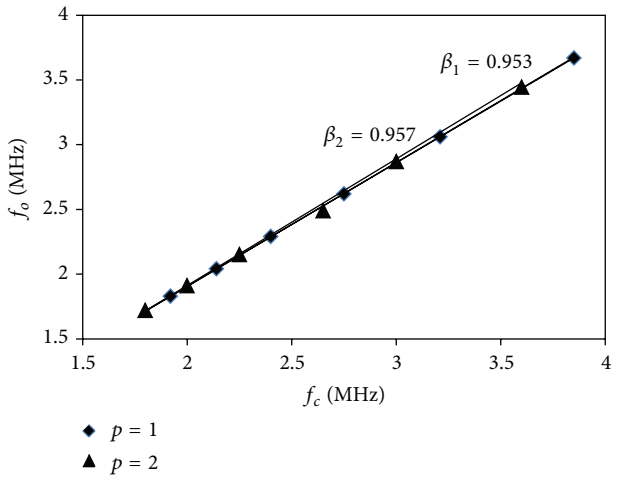

FIGURE 5: Variation of the S_1-ZGV frequency f_o versus the cut-off frequency f_c for different values of p.

That is still true for a nonlinear profile. Accordingly the S_1-ZGV frequency reveals a high sensitivity either to the metal shear modulus or to the plate thickness. That result can be exploited in the study of the microsystems.

4.3. Effect of FGM Proprieties on the Shape Factor β. For a homogenous plate, it has been shown that the S_1-ZGV frequency f_o varies linearly with the cut-off frequency (f_c) according to the relation $f_o = \beta * f_c$, where β is the shape factor introduced by Sansalone et al. [23, 24].

These ZGV and cut-off frequencies are studied when the plate thickness of FGM plate is increased from d to $2d$. For the nonlinear profile of the FGM plate, the obtained results reveal that the ZGV frequency f_o presents the same behavior; a linear variation in terms of the cut-off frequency is reported in Figure 5. The obtained linear variation in the case of the nonlinear FGM plate seems to be in agreement with the literature [14]. The gradient coefficient p does not affect the linear dependence of f_o as function of f_c, but β varies slightly (see Figure 5).

Moreover, β undergoes slight change when p varies from 1 to 2. That is mainly produced by a small change of the Poisson's ratio υ due to its local character. To illustrate how f_o depends on f_c, two kinds of FGM plates have been selected Cr/ceramic and Ni/ceramic. For the first couple, ν_{Cr} is smaller than $\nu_{Ceramic}$ whereas, for the second couple, ν_{Ni} is greater than $\nu_{Ceramic}$. The reported shift in Figure 5 is coherent with the corresponding Poisson's ratios. The obtained result is consistent with the relationship of β according to ν, given by Clorennec [4].

4.4. Mechanical Displacement and Distribution of Stress. At the dispersive region of the S_1 mode, the phase velocity decreases rapidly when the frequency passes from f_c to f_o and the guided wave leaves its steady character. At the cut-off frequency (f_c), the whole surface is vibrating in phase. Conversely, with a finite wave number, ZGV modes give rise to local resonances. So, we focus on this resonance frequency f_o to study the vibratory structure of the S_1 Lamb modes in the FGM plate. In Figure 6, the variation of the stress and the mechanical displacement are plotted as function of the depth at the f_o frequency.

Using the mechanical displacements $U_1(x_3)$ and $U_3(x_3)$ plotted in Figure 6(a), we can describe the wave power penetration through the thickness of FGM plate. Because of the asymmetric properties of the FGM plate, the displacement

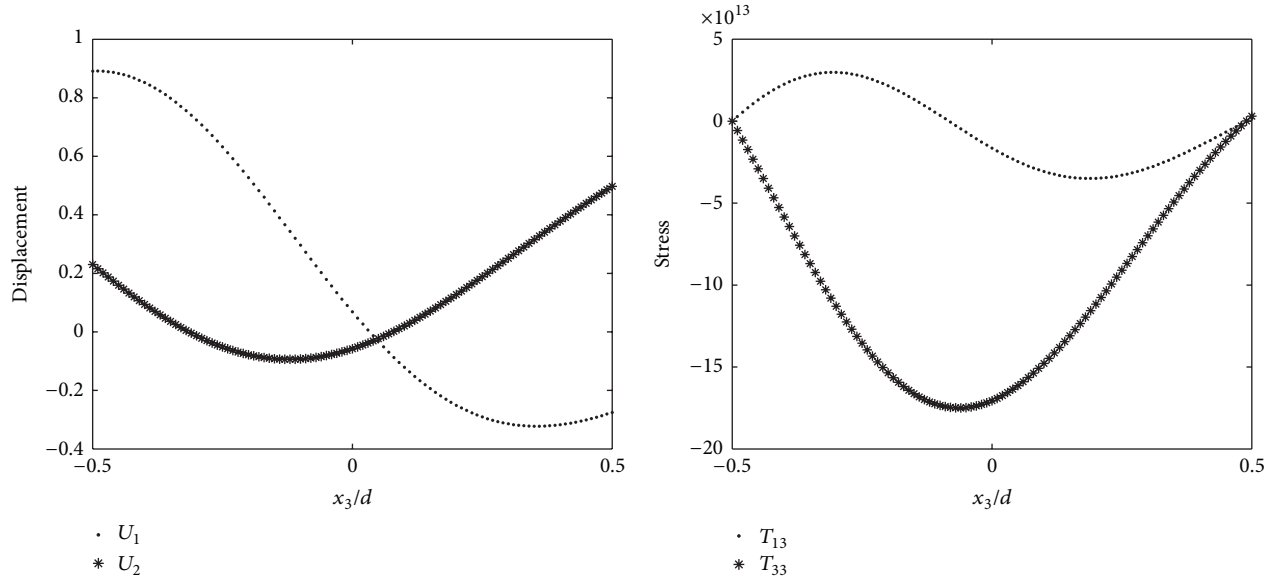

Figure 6: Profiles of displacement (a) and stress (b) in the nonlinear ceramic-chromium FGM plate.

amplitudes do not reveal a symmetric character as obtained for the homogeneous plate [3, 20]. The amplitudes of U_1 and U_3 are comparatively high in the neighborhood of the free surfaces. The obtained profiles for the longitudinal and the transverse components, respectively, U_1 and U_3 are coherent with the symmetrical character of the ZGV mode.

Besides we verify on Figure 6(b) that stress components T_{13} and T_{33} vanish on free sides of the FGM plate. This permits to be ensured about the computation process. The same plots performed for the linear FGM profile [16], not included here, show that displacement components are more sensitive than stress components to p coefficient.

5. Conclusion

Using the power series technique, we have analytically solved the propagation of Lamb waves. As an originating phenomenon, the S_1-ZGV Lamb mode in a functionally graded plate is studied. Based on the PST, governing equations for the problem of Lamb waves that propagate in an FGM plate are derived. For the kinds of FGM discussed in this paper, the S_1-ZGV frequency in an FGM plate is between those for the two corresponding homogeneous plates. Moreover, the S_1-ZGV value depends on metal shear modulus and gradient coefficient p.

Hence, in both cases (linear and nonlinear), the metal shear modulus influences enormously the S_1-ZGV.

On the other hand, the linear dependence between S_1-ZGV frequency f_o and cut-off frequency f_c is still observed even for nonlinear profile. The ZGV frequency provides a local measurement of Poisson's ratio. At the point corresponding to ZGV frequency, the displacement components are more sensitive than stress components.

Conflict of Interests

The authors declare that there is no conflict of interests regarding the publication of this paper.

References

[1] J. L. Rose, *Ultrasonic Waves in Solid Media*, Cambridge University Press, New York, NY, USA, 1999.

[2] D. Clorennec, C. Prada, and D. Royer, "Local and noncontact measurements of bulk acoustic wave velocities in thin isotropic plates and shells using zero group velocity Lamb modes," *Journal of Applied Physics*, vol. 101, Article ID 034908, 2007.

[3] M. Cès, D. Clorennec, D. Royer, and C. Prada, "Thin layer thickness measurements by zero group velocity Lamb mode resonances," *Review of Scientific Instruments*, vol. 82, no. 11, Article ID 114902, 2011.

[4] I. Tolstoy and E. Usdin, "Wave propagation in elastic plates: low and high mode dispersion," *The Journal of the Acoustical Society of America*, vol. 29, pp. 37–42, 1957.

[5] S. D. Holland and D. E. Chimenti, "Air-coupled acoustic imaging with zero-group-velocity Lamb modes," *Applied Physics Letters*, vol. 83, no. 13, pp. 2704–2706, 2003.

[6] C. Prada, D. Clorennec, and D. Royer, "Local vibration of an elastic plate and zero-group velocity Lamb modes," *Journal of the Acoustical Society of America*, vol. 124, no. 1, pp. 203–212, 2008.

[7] D. Clorennec, C. Prada, and D. Royer, "Laser ultrasonic inspection of plates using zero-group velocity lamb modes," *IEEE Transactions on Ultrasonics, Ferroelectrics, and Frequency Control*, vol. 57, no. 5, pp. 1125–1132, 2010.

[8] G. R. Liu, X. Han, and K. Y. Lam, "An integration technique for evaluating confluent hypergeometric functions and its application to functionally graded materials," *Computers & Structures*, vol. 79, no. 10, pp. 1039–1047, 2001.

[9] X. Han, G. R. Liu, K. Y. Lam, and T. Ohyoshi, "Quadratic layer element for analyzing stress waves in FGMS and its application in material characterization," *Journal of Sound and Vibration*, vol. 236, no. 2, pp. 307–321, 2000.

[10] X. Han and G. R. Liu, "Elastic waves in a functionally graded piezoelectric cylinder," *Smart Materials and Structures*, vol. 12, no. 6, pp. 962–971, 2003.

[11] Z. H. Qian, F. Jin, Z. K. Wang, and K. Kishimoto, "Transverse surface waves on a piezoelectric material carrying a functionally graded layer of finite thickness," *International Journal of Engineering Science*, vol. 45, pp. 455–466, 2007.

[12] X. Y. Li, Z. K. Wang, and S. H. Huang, "Love waves in functionally graded piezoelectric materials," *International Journal of Solids and Structures*, vol. 41, no. 26, pp. 7309–7328, 2004.

[13] V. Vlasie and M. Rousseau, "Guided modes in a plane elastic layer with gradually continuous acoustic properties," *NDT and E International*, vol. 37, no. 8, pp. 633–644, 2004.

[14] J. Liu and Z. Wang, "Study of the propagation of Rayleigh surface waves in a graded half-space," *Chinese Journal of Applied Mechanics*, vol. 21, pp. 106–109, 2004.

[15] X. Cao, F. Jin, and I. Jeon, "Calculation of propagation properties of Lamb waves in a functionally graded material (FGM) plate by power series technique," *NDT and E International*, vol. 44, no. 1, pp. 84–92, 2011.

[16] M. S. Bouhdima, M. Zagrouba, and M. H. Ben Ghozlen, "The power series technique and detection of zero-group velocity Lamb waves in a functionally graded material plate," *Canadian Journal of Physics*, vol. 90, no. 2, pp. 159–164, 2012.

[17] C. Prada, O. Balogun, and T. W. Murray, "Laser-based ultrasonic generation and detection of zero-group velocity Lamb waves in thin plates," *Applied Physics Letters*, vol. 87, no. 19, Article ID 194109, 2005.

[18] J. N. Reddy and C. D. Chin, "Thermomechanical analysis of functionally graded cylinders and plates," *Journal of Thermal Stresses*, vol. 21, no. 6, pp. 593–626, 1998.

[19] J. N. Reddy, C. N. Wang, and S. Kitipornchai, "Axisymetric bending of functionally graded circular and annular plate," *European Journal of Mechanics—A/Solids*, vol. 18, pp. 185–199, 1999.

[20] Z.-Q. Cheng and R. C. Batra, "Three-dimensional thermoelastic deformations of a functionally graded elliptic plate," *Composites B: Engineering*, vol. 31, no. 2, pp. 97–106, 2000.

[21] J. Woo and S. A. Maguid, "Nonlinear analysis of functionally graded plates and shallow shells," *International Journal of Solids and Structures*, vol. 38, pp. 7409–7421, 2001.

[22] L. S. Ma and T. J. Wang, "Nonlinear bending and post-buckling of a functionally graded circular plate under mechanical and thermal loadings," *International Journal of Solids and Structures*, vol. 40, no. 13-14, pp. 3311–3330, 2003.

[23] M. Sansalone and N. J. Carino, "National Bureau of Standards," Report NBSIR 86-3452, NBSIR, Gaithersburg, Md, USA, 1986.

[24] A. Gibson and J. S. Popovics, "Lamb wave basis for impact-echo method analysis," *Journal of Engineering Mechanics*, vol. 131, no. 4, pp. 438–443, 2005.